

# The dark matter potential and the evolution of dwarf spheroidal galaxies

M. M. de Castro<sup>1</sup>, G. A. Lanfranchi<sup>1</sup> & A. Caproni<sup>1</sup>

<sup>1</sup> Núcleo de Astrofísica – NAT, Universidade Cidade de São Paulo e-mail: gustavo.lanfranchi@cruzeirosul.edu.br

**Abstract.** The proximity and the particular characteristics of Local Group Dwarf Galaxies make them important objects in the study of galactic evolution. Local Dwarf Spheroidals, for example, exhibit particular chemical properties and total absence of neutral gas. The process responsible for the removal of their gaseous content is a matter of debate in the literature: it could be internal (stellar feedback), external (ram-pressure, tidal stripping), or a combination of both. Either way, the gravitational potential of the galaxy plays an important role in gas loss, binding the gas to the system, and an important component of the potential is the dark matter halo that dominates it. Gas removal in Dwarf Spheroidal Galaxies is investigated, taking into account different configurations for the dark matter halo, by means of a three-dimensional hydrodynamic simulation code already applied for the Ursa Minor galaxy. All other parameters of the initial setup of the code are kept the same. In this way we can better understand how the gas from these galaxies has been exhausted and what is the role of the dark matter halo in this process.

**Resumo.** A proximidade e as características particulares das Galáxias Anãs do Grupo Local as tornam objetos chave nos estudos de evolução galáctica. As Galáxias Anãs Esferoidais, por exemplo, apresentam propriedades químicas particulares e total ausência de gás. O processo responsável pela remoção do gás, entretanto, ainda não é conhecido: ele pode ser interno (*feedback* estelar), externo (pressão de maré, força de arrasto) ou uma combinação dos dois. Qualquer que seja o processo, o potencial gravitacional da galáxia tem um papel importante na perda de gás, aprisionando-o à galáxia, e um componente importante do potencial é o halo de matéria escura, que o domina. A remoção do gás em Galáxias Esferoidais Anãs é investigado, levando em conta diferentes configurações para o halo de matéria escura, através de um código hidrodinâmico tridimensional já aplicado à galáxia Ursa Minor. Todos os outros parâmetros das configurações iniciais do códigos são mantidos iguais. Dessa maneira, será possível entender melhor como o gás dessas galáxias foi removido e qual o papel desempenhado pelo halo de matéria escura nesse processo.

**Keywords.** Galaxies: dwarf – Galaxies: evolution – Hydrodynamics

## 1. Introduction

The Dwarf Spheroidal Galaxies (dSph) have small dimensions, ( $R_T \sim 2 - 6$  kpc), low luminosity ( $M_V = -14$  mag.), low masses ( $M \sim 10^7 M_\odot$ ) and are metal-poor ( $[Fe/H] = -2.5$  to  $-1.0$ ) (Tolstoy, Hill & Tosi 2009). They have no nucleus or significant central concentrations of stars, are characterized by ancient stellar populations ( $> 10$  Gyr) and intermediate age stars (1-10 Gyr). The star formation has already ended several Gyr, but some dSphs show signs of more extended activity. The most intriguing feature of the dSphs is the absence of neutral gas in their central region, whose cause remains unsolved: it is not known whether the removal of the gas was caused by internal or external mechanisms.

In classical Local Group dSph galaxies, the estimated mass-luminosity ratio is as higher as 100, and there is an apparent relationship between this ratio and the luminosity of the galaxy: the lower the luminosity, the greater the M-L value (Walker et al. 2010). However, the exact amount of dark matter and the shape of the dark matter potential are still not known with accuracy. There is a debate whether the density of dark matter in dwarf galaxies is approximately constant in the central regions - cuspy profile (Diemand et al. 2005) or behaves as an intense potential law - cored profile - at scales exceeding a few hundred parsec (Gilmore et al. 2007).

## 2. Results

The effects of the dark matter halo on the dynamics of the gaseous content of local Dwarf Spheroidal Galaxies started to be analyzed by adopting different amounts of dark matter halos in these systems with the use of a three-dimensional hydrody-

namic code - PLUTO - already used by the group (CAPRONI et al. 2015, 2017). The initial code settings are the same as those used for the dSph Ursa Minor galaxy. The evolution of the gas content of the galaxy is followed for 1 Gyr, inside a 3.6 kpc computational box, divided in  $60^3$  cells.

Two simulations were performed with the same values for almost all parameters, but with different masses for the dark matter component. The amount of dark matter is constrained by the circular velocity and the initial gas mass is related to the dark matter mass by the relation between baryonic mass and dark matter as derived by the WMAP. The reference simulation (VC21) adopts the circular velocity  $v_c = 21.1 \text{ km.s}^{-1}$  (Strigari et al. 2008) resulting in an initial gas mass  $M_{g0} = 5.99 \times 10^8 M_\odot$  and a dark matter halo mass  $M_h = 3.05 \times 10^9 M_\odot$ , constant throughout the simulation. A second simulation (VC38) with a higher mass of dark matter adopts the higher limit of the circular velocity  $v_c = 38.0 \text{ km.s}^{-1}$  yielding  $M_h = 1.82 \times 10^{10} M_\odot$ . In this case the ratio between dark and luminous matter was changed in order to maintain the same initial gas mass as in VC21.

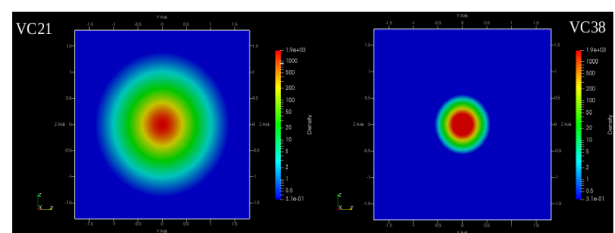


**FIGURE 1.** Cut in the zy plane of the density profile at  $t = 0$  yr for simulations VC21 (left) and VC38 (right).

At the beginning of the simulations,  $t = 0$  yr, the gas is in hydrostatic equilibrium with the dark matter potential and the gas density profile in the case of VC38 exhibits a higher concentration of barionic matter compared to VC21 case (right and left, respectively, in Figure 1). The higher concentration is caused by the higher dark matter mass, the main component of the gravitational potential of the galaxy.

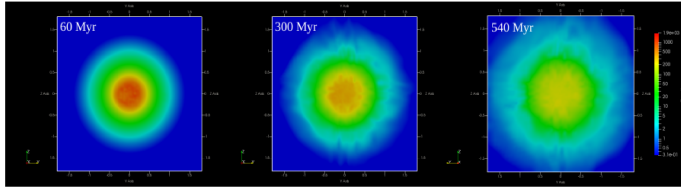


**FIGURE 2.** Cut in the zy plane of the gas density profile at 60 Myr, 300 Myr, and 540 Myr for simulation VC21.

Starting from the equilibrium, the energy of SNe is injected in the ISM of the galaxy according to the SNe rate of Lanfranchi & Matteucci (2010). At  $t = 60$  Myr, the effects of SNe on the gas are not visible in VC38 (Figure 3) due to the high density of the medium. In the case of VC21 (Figure 2), the SNe already decreased the central initial density. At  $t = 300$  Myr, the central gas density is even smaller in VC21 and the gas is expanding. In the case of VC38, the effects of SNe start to appear at the external regions. At  $t = 540$  Myr, in VC21 low density gas occupies almost all the region, whereas in VC38 it remains constrained within 500 pc, with noticeable perturbations.

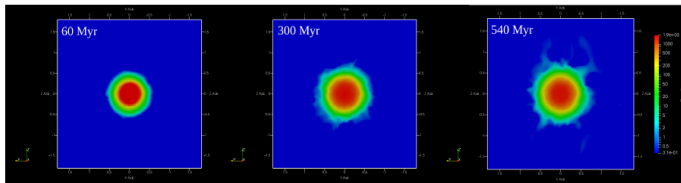


**FIGURE 3.** Cut in the zy plane of the gas density profile at 60 Myr, 300 Myr, and 540 Myr for simulation VC38.

The different evolution of the gas density across the galaxy in the two simulations leads also to a different spatial distribution of SNe II, since the sites for the occurrence of these supernovae depends on the density. When the mass of dark matter is higher (VC38) the SNe II are more concentrated (Figure 4) remaining inside a radius of almost 200 pc.

The comparison between the remaining gas inside different regions of the galaxy for both simulations shows that the case with a more massive dark matter component loses less gas. At 540 Myr, less than 5% of the initial gas mass inside the tidal radius of the galaxy in the simulation VC38 was lost (continuous red line in Figure 5), whereas almost 20% was lost in the simulation with a less massive dark matter halo (VC21 - dotted red line in Figure 5). The same scenario holds at the central region of the galaxy (300 pc - black lines in Figure 5); whereas VC38 simulation retains  $\sim 55\%$  of its initial gas, the simulation with a less massive dark halo retains only almost 20%.

### 3. Conclusion

The VC38 simulation, with the most massive halo, shows lower mass loss. The dark matter potential changes the initial distribution of gas: the concentration of gas is higher when the

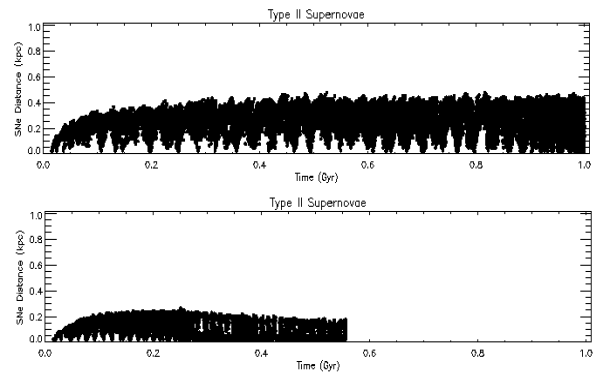


**FIGURE 4.** Distance of site of occurrence of each SNe II to the center of the galaxy as a function of time for simulation VC21 (top) and VC38 (bottom).

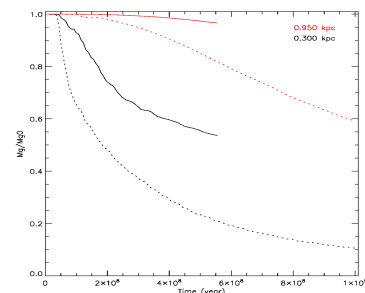


**FIGURE 5.** Fraction of initial mass remaining within different spherical regions of the galaxy (black line - 300 pc, red 950 pc, in simulations VC21 (dotted line) and VC38 (continuous line).

dark halo is more massive; the spatial distribution of SNe II: the higher central density of gas in the VC38 simulation constrains the SNe II within 200 pc radius; and defines the depth of the potential well of the galaxy. The deeper potential well of the simulation with a large dark matter mass (VC38) allied to the more concentrated distribution of SNe II makes it more difficult for the gas to leave the galaxy. At the end of 540 Myr the galaxy with a large dark matter mass (6 times higher) loses 4 times less gas at its tidal radius than the galaxy with less dark matter.

*Acknowledgements.* This work has made use of the Sistema de Computação Petaflopica do SINAPAD — Laboratório Nacional de Computação Científica (LNCC). The authors thank the Brazilian agency CNPq (grant 304928/2015-1), FAPESP (grants 2014/11156-4, 2017/25651-5 and 2017/25799-2), and CAPES.

### References

- Caproni A., Lanfranchi G. A., da Silva A. Luiz, Falceta-Gonçalves D., 2015, ApJ, 805, 109
- Caproni, A. Lanfranchi, G. A.; Baio, G. H. C.; Kowal, G.; Falceta-Gonçalves, D. 2017, ApJ, 838, 99
- Diemand, J., Zemp, M., Moore, B., Stadel, J., & Carollo, C. M. 2005, MNRAS, 364, 665
- Gilmore G., Wilkinson M. I., Wyse R. F. G., Kleyna J. T., Koch A., Evans N. W., Grebel E. K., 2007, ApJ, 663, 948
- Lanfranchi G. & Matteucci F., 2010, A&A, 512, A85
- Strigari, L. E., et al., 2008, Nature, 454, 1096.
- Tolstoy, E., Hill, V., Tosi, M., 2009, ARA&A, 47, 371
- Walker, M.G.; McGaugh, S.S.; Mateo, M.; Olszewski, E. W.; Kuzio de Naray, R., 2010, ApJ, 717, 87